RSC Advances

ROYAL SOCIETY OF CHEMISTRY

www.rsc.org/advances

Spectroscopic characterization of C-4 substituted 3,5-dichloro-4*H*-1,2,6-thiadiazines

Eleni Theodorou, Heraklidia A. Ioannidou, Theodosia A. Ioannou, Andreas S. Kalogirou, Christos P. Constantinides, Maria Manoli, Panayiotis A. Koutentis, and Sophia C. Hayes**

Department of Chemistry, University of Cyprus, P.O. Box 20537, 1678, Nicosia, Cyprus

e-mail: koutenti@ucy.ac.cy, shayes@ucy.ac.cy

Three 3,5-dichloro-4*H*-1,2,6-thiadiazines, which differ according to the electron withdrawing nature of their substituent at C-4: (a) 3,5-dichloro-4-methylene-4*H*-1,2,6-thiadiazine (**5a**), (b) 3,5-dichloro-4*H*-1,2,6-thiadiazin-4-one (**5b**) and (c) 2-(3,5-dichloro-4*H*-1,2,6-thiadiazin-4-ylidene)malononitrile (**5c**), are characterized using resonance Raman (RR), absorption (UV/vis) and photoluminescence (PL) spectroscopies. These weakly aromatic and electron-deficient heterocycles are potential components as acceptors in donor-acceptor systems for organic electronics. Experimental results, which include the synthesis, characterization and single crystal X-ray structure of 3,5-dichloro-4-methylene-4*H*-1,2,6-thiadiazine (**5a**), combined with theoretical calculations of their orbitals and vibrational frequencies, provide an understanding of the optical properties, on the basis of molecular geometry and electron distribution.

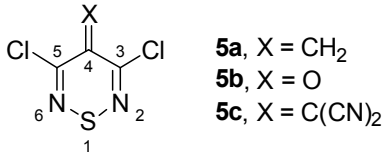

5a, X = CH_2
5b, X = O
5c, X = $C(CN)_2$

1. Introduction

Heteroaromatic compounds have many uses in diverse fields such as the pharmaceutical, agrochemical and materials sectors.[1] π-Conjugated small molecules, oligomers and polymers, that are composed of heteroaromatic compounds *e.g.*, pyrroles, carbazoles and thiophenes, have been successfully used in organic electronic devices.[2] The recent successes and the demand for more efficient optoelectronic devices have led to an intense search for new materials with improved physicochemical and electronic properties.

Within the field of heterocyclic chemistry there are a number of potentially useful scaffolds that have yet to be exploited and have essentially remained dormant since they were first reported. One such scaffold is 3,5-dichloro-4*H*-1,2,6-thiadiazin-4-one, which was first reported in 1974.[3] For over twenty years the chemistry of this scaffold has been limited to the substitution of a chlorine, and the monochloro-monosubstituted thiadiazines have been studied as antifungal agents.[4] Nevertheless, a recent perspective on R. B. Woodward's "unfinished symphony" identified poly(1,2,6-thiadiazines) as potential stable alternatives to the superconductor poly(sulfur nitride) $(SN)_x$.[5] A similar proposal was later put forward by C. W. Rees (Fig. 1).[6-8]

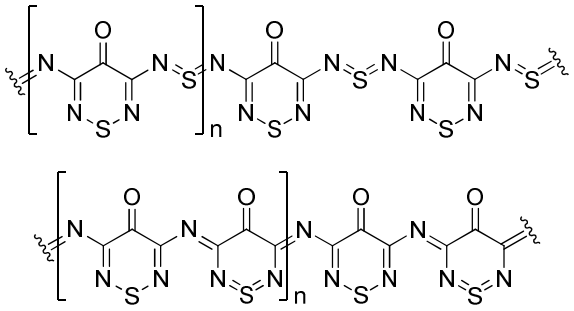

Fig. 1 1,2,6-Thiadiazinone polymers proposed as alternatives to poly(sulfur nitride) $(SN)_x$ by Woodward (top) and Rees (bottom).

In addition, several fused 4*H*-1,2,6-thiadiazines such as acenaphtho[5,6-*cd*][1,2,6]thiadiazine (**1**),[9,10] and naphtho[1,8-*cd*:4,5-*c'd'*]bis([1,2,6]thiadiazine) (**2**),[11] have been studied as examples of 'extreme quinoids' that have ambiguous aromatic character, while Torroba *et al.*,[12,13] prepared cyclopenta[1,2,6]thiadiazines **3** and **4** starting from cyclic enaminonitriles, some of which displayed unusual liquid crystalline properties or behaved as near infra-red dyes (Fig. 2).

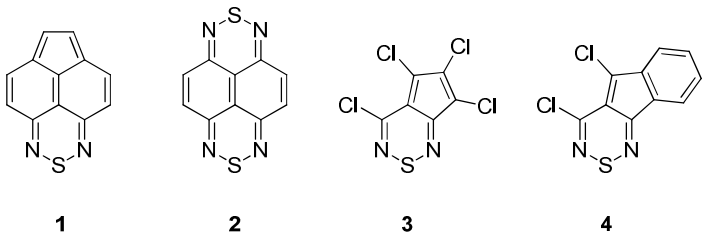

Fig. 2 Selected fused 4*H*-1,2,6-thiadiazines.

Since 2000, we have been developing the synthesis and chemistry of 4*H*-1,2,6-thiadiazines,[6-8, 14-18] which has led to the preparation of the dicyanomethylene analogue **5c**, on treating tetracyanoethene (TCNE) with sulfur dichloride.[6, 8] Recently, an electrochemical study of a diverse library of 1,2,6-thiadiazines indicated the dicyanomethylenes had electron affinities of 3.8-4.0 eV that were suitable as electron acceptor components for organic photovoltaic devices,[19] while organic solar cells containing small molecule donors incorporating 1,2,6-thiadiazinones have already led to PCE of ~2.7%.[20] Despite the potential applications, detailed spectroscopic studies of these compounds have not yet appeared in the literature. Below we report the preparation of 3,5-dichloro-4-methylene-4*H*-1,2,6-thiadiazine (**5a**) for the first time. With this compound in hand we have access to three 3,5-dichloro-4*H*-1,2,6-thiadiazines that vary at the C-4 position (Fig. 3), allowing us to study the influence of the electron withdrawing power of the C-4 substituent on the structure and electronic properties of the ring system.

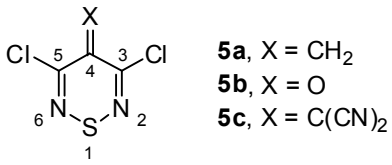

Fig. 3 Chemical structure of 3,5-dichloro-4-methylene-4*H*-1,2,6-thiadiazine (**5a**), 3,5-dichloro-4*H*-1,2,6-thiadiazin-4-one (**5b**) and 2-(3,5-dichloro-4*H*-1,2,6-thiadiazin-4-ylidene)-malononitrile (**5c**) together with the IUPAC numbering system for the heterocycle.

2. Results and Discussion

2.1. Synthesis

Thiadiazines **5b**[3] and **5c**[7,8] were prepared according to literature methods starting from dichloromalononitrile and TCNE, respectively. The 3,5-dichloro-4-methylene-4*H*-1,2,6-

thiadiazine (**5a**) was prepared by reacting the dichlorothiadiazinone **5b** with methylmagnesium bromide (2 equiv.) in diethyl ether at -78 °C for 15 min followed by treatment with $TsOH \cdot H_2O$ (5 mol %) in toluene heated to *ca.* 110 °C (Scheme 1).

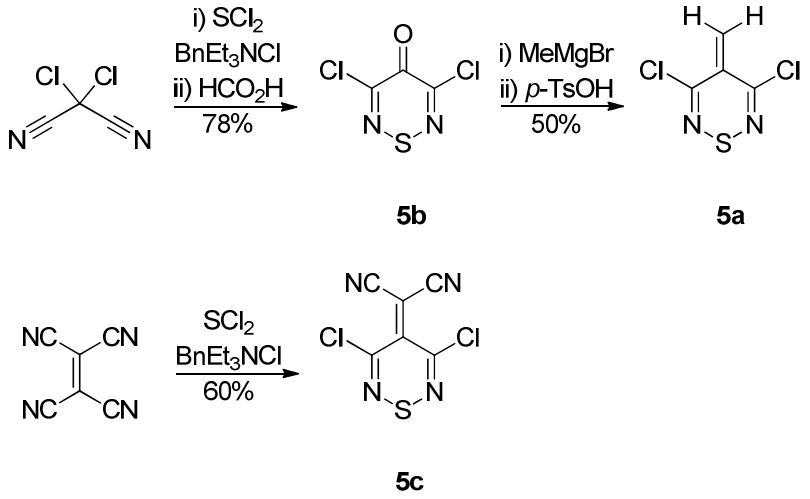

Scheme 1 Synthesis of 4*H*-1,2,6-thiadiazines **5a**, **5b** and **5c**.

The methylene thiadiazine **5a** was isolated as yellow needles, mp 73-75 °C (from *n*-pentane) and showed a lower wavelength absorption in the UV/vis [λ_{max}(DCM)/nm 309 (log ε 3.72)] than that recorded for the analogous thiadiazinone **5b** [λ_{max}(DCM)/nm 326 (log ε 4.38)] and the ylidenemalonitrile **5c** [λ_{max}(DCM)/nm 403 (log ε 4.38)][8] analogues (Figure 5), suggesting a less delocalized system (see below). This was further supported by the compound's poor stability in the solid state. A pale yellow crystalline sample of the methylene **5a** stored at room temperature gradually became orange and then red and on analysis (TLC) had decomposed showing no traces of the starting methylene **5a**. Instead, a strong odor of sulfur chlorides was detected and TLC analysis showed several very minor products but interestingly little sulfur. This unexpected decomposition is currently under investigation and a detailed study will be reported in the near future.

In light of this instability, we prepared single crystals of the methylene **5a** *via* slow cooling of a *n*-pentane solution and obtained a crystallographic structure (Fig. 4) allowing a bond length and bond angle analysis for comparison to the known X-ray structures of the analogous thiadiazinone **5b**[21] and ylidenemalononitrile **5c**.[6] While the thiadiazinone **5b** was almost planar,[21] the analogous methylene **5a** deviated slightly from planarity but not to the extent

displayed by the dicyanomethylene **5c**.[6] Tentatively, this deviation can be attributed to steric interactions between the thiadiazines 3,5-chlorines and the C-4 substituents.

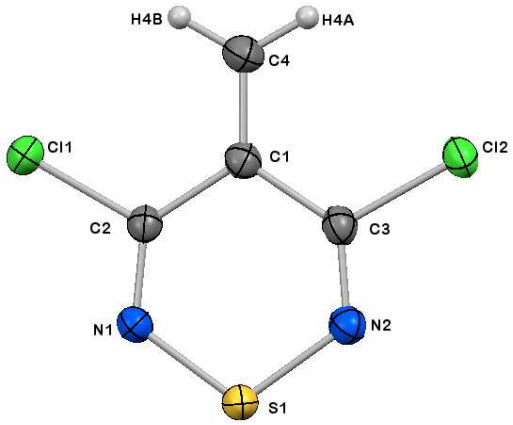

Fig. 4 Ortep representation of the single crystal X-ray structure of 3,5-dichloro-4-methylene-4*H*-1,2,6-thiadiazine (**5a**) with crystallographic atom labelling.

2.2. Optical properties

Fig. 5 presents absorption spectra of the three compounds of interest measured in DCM solution. The methylene thiadiazine **5a** (X = CH_2) shows an absorption band at 309 nm, while the absorption spectrum of the thiadiazinone **5b** (X = O) is broad with clear contributions from two transitions, with a λ_{max} at 290 and 326 nm. The absorption spectrum of the dicyanomethylene **5c** [X = $C(CN)_2$] is unstructured, broad and significantly red-shifted relative to the other two molecules, with a λ_{max} at 404 nm, consistent with increased electron delocalization. The fluorescence spectrum of the methylene thiadiazine **5a** (λ_{max} = 376 nm) (Fig. 6) appears slightly broader than in the case of the thiadiazinone **5b** (λ_{max} = 373 nm), with weak vibronic structure. In the case of the dicyanomethylene **5c**, the fluorescence spectrum is broader with a λ_{max} at 473 nm, appreciably red-shifted relative to the other two molecules as also observed in absorption. In addition, the fluorescence intensity of the latter molecule is larger, pointing to a higher quantum yield, as evidenced by the larger noise in the normalized spectra of thiadiazines **5a** and **5b**.

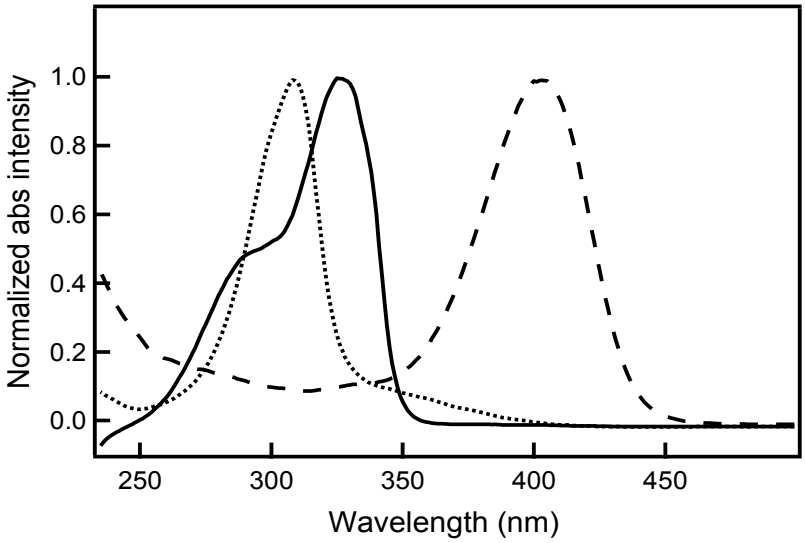

Fig. 5 Normalized absorption spectra of the thiadiazines **5a** (X = CH_2) (dotted line), **5b** (X = O) (black line) and **5c** [X = $C(CN)_2$] (dashed line).

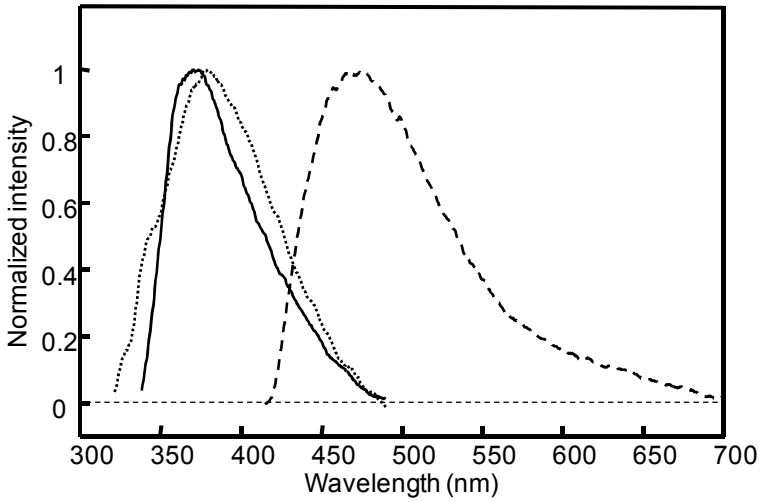

Fig. 6 Normalized photoluminescence spectra of the thiadiazines **5a** (X = CH_2) (dotted line), **5b** (X = O) (solid line) and **5c** [X = $C(CN)_2$] (dashed line) with excitation at $\lambda_{abs,max}$.

Insight into the optical properties of molecules **5a-c** was derived from theoretical calculations of the frontier molecular orbitals. The HOMO and LUMO energy levels, as well as their spatial distributions are crucial parameters for determining the molecular electronic properties.[22] The geometrical structures were fully optimized in their ground state at the MP2/6-311G(d) level of theory (Fig. 7). In agreement with the X-ray structure,[6] the

dicyanomethylene **5c** adopted a shallow boat conformation in its optimized ground state geometry in contrast to compounds **5a** and **5b** that exhibited planar conformations. However, the dihedral angle between the planes defined by the C3-C4-C5 and the C3-N2-N6-C5 atoms (see Fig. 3) in **5c** is 15.3°, while the angle between planes defined from the N2-S1-N6 atoms and the C3-N2-N6-C5 atoms is 8.7°. These measurements suggest there is sufficient π orbital overlap to consider the ring system to be weakly aromatic (see below).

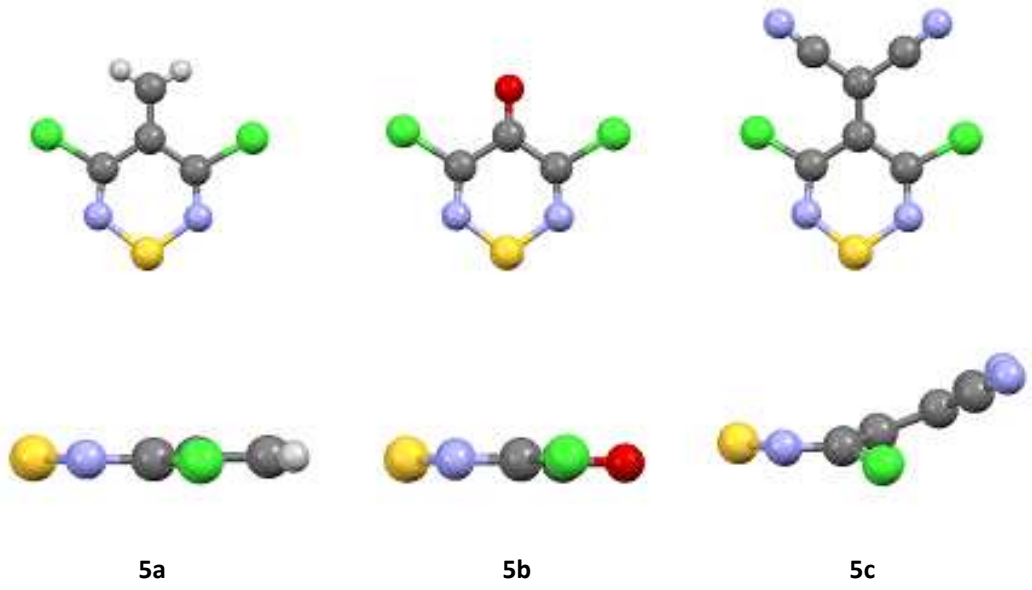

Fig. 7 The optimized lowest energy structures of the ground state of 4*H*-1,2,6-thiadiazines **5a**, **5b** and **5c** at the MP2/6-311G(d) level of theory calculated using Gaussian (top view: above ring plane; bottom view: in plane).

Table 1 summarizes the dominant transitions, vertical transition energies calculated using the TD-DFT/B3LYP/6-311+G(2d) method on MP2/6-311G(d) optimized structures, the corresponding assignments of the experimental absorption spectra, and oscillator strengths for all three compounds. Closely-spaced transitions are calculated for all three compounds. For the methylene **5a**, the major transitions (with the highest oscillator strength) are the HOMO → LUMO (45 → 46) and the HOMO → LUMO+1 (45 → 47), with vertical excitation energies 4.15 and 3.63 eV (4.01 and 3.49 eV experimental values, respectively, assigned based on the oscillator strength of the two transitions). Interestingly, the calculated vertical excitation energy for the HOMO → LUMO+1 appears at a lower energy than the transition assigned to the HOMO → LUMO. Computations using a variety of basis sets have reproduced this result, which suggests that additional terms (such as two-electron integrals) in

addition to the energy difference between orbitals participating in the transition along with probably a mixture of electronic configurations describing the excited state, contribute to this vertical excitation energy, raising thus the energy of the HOMO → LUMO transition.[23] This is not observed for the other two compounds. For the thiadiazinone **5b**, the two major transitions are the HOMO → LUMO (45 → 46) and the HOMO → LUMO+1 (45 → 47) with vertical excitation energies 3.99 and 4.37 eV, and oscillator strengths 0.1491 and 0.1277, respectively. These transitions agree with the experimental energies of the bands in the absorption spectrum, where we observe transition to two states, one at 3.80 and the other at 4.27 eV. Three major transitions are calculated in the case of the dicyanomethylene **5c** the HOMO → LUMO (57 → 58) with ΔE = 3.16 eV, the HOMO → LUMO+1 (57 → 59) with ΔE = 3.71 eV and the HOMO-2 → LUMO (55 → 58) with ΔE = 4.47 eV. This is confirmed from the absorption spectrum of the molecule (Fig. 5).

Fig. 8 presents the frontier orbitals involved in the electronic transitions described in Table 4 for the three compounds. Despite the different substitution at C-4 for the thiadiazines **5a** and **5b**, their frontier orbital diagrams appear very similar. A difference is observed, though, in their HOMO orbitals, where in the thiadiazinone **5b** the electron density is delocalized throughout the N=C-C-C=N moiety, while there is a node in the C-C bonds in the methylene **5a** consistent with a more quinoidal structure. A further difference exists between the orbitals of thiadiazines **5a** and **5b** and those that correspond to the dicyanomethylene **5c**, where electron density appears throughout the molecule, owing to the extended π-conjugated system offered by the $=C(CN)_2$ group. This is consistent with increased delocalization of the electron cloud and aromaticity of the ring (see below) as evidenced by the red-shift in the absorption spectrum and supported by the vertical excitation calculations. Observation of the electronic density contours of these orbitals identifies the HOMO – LUMO and the HOMO – LUMO+1 transitions as π-π^* in all cases.

Table 1 Calculated electronic transitions, vertical excitation energies and their assignments for compounds **5a-c** using the TD-DFT/B3LYP/6-311+G(2d) method on MP2/6-311G(d) optimized structures

State	Transitions	ΔE (eV)	ΔE_{exp} (eV)	ΔE_{exp} (nm)	f
5a					
1A	**45 → 47 (0.70) (H→L+1)**	3.63	3.49	355	0.0264
2A	**45 → 46 (0.69) (H→L)**	4.15	4.01	309	0.2740
3A	44 → 46 (0.70)	4.57			0.0000
4A	44 → 47 (0.70)	4.82			0.0035
5A	45 → 48 (0.70)	4.98			0.0001
6A	45 → 49 (0.70)	5.00			0.0000
5b					
1A	44 → 46 (0.70)	3.00			0.0000
2A	**45 → 46 (0.69) (H→L)**	3.99	3.80	326	0.1491
3A	44 → 47 (0.70)	4.03			0.0006
4A	**45 → 47 (0.69) (H→L+1)**	4.37	4.27	290	0.1277
5A	40 → 46 (0.24) 42 → 46 (0.66)	4.88			0.0000
6A	40 → 46 (0.66)	4.92			0.0000
5c					
1A	**57 → 58 (0.69) (H→L)**	3.16	3.07	404	0.2932
2A	**57 → 59 (0.70) (H→L+1)**	3.71	3.71	334	0.0250
3A	54 → 58 (0.27) 56 → 58 (0.64)	3.99			0.0057
4A	54 → 58 (0.64)	4.21			0.0018
5A	55 → 58 (0.57) 57 → 58 (0.13)	4.47	4.52	274	0.1099
6A	53 → 58 (0.61) 55 → 58 (0.20)	4.56			0.0028

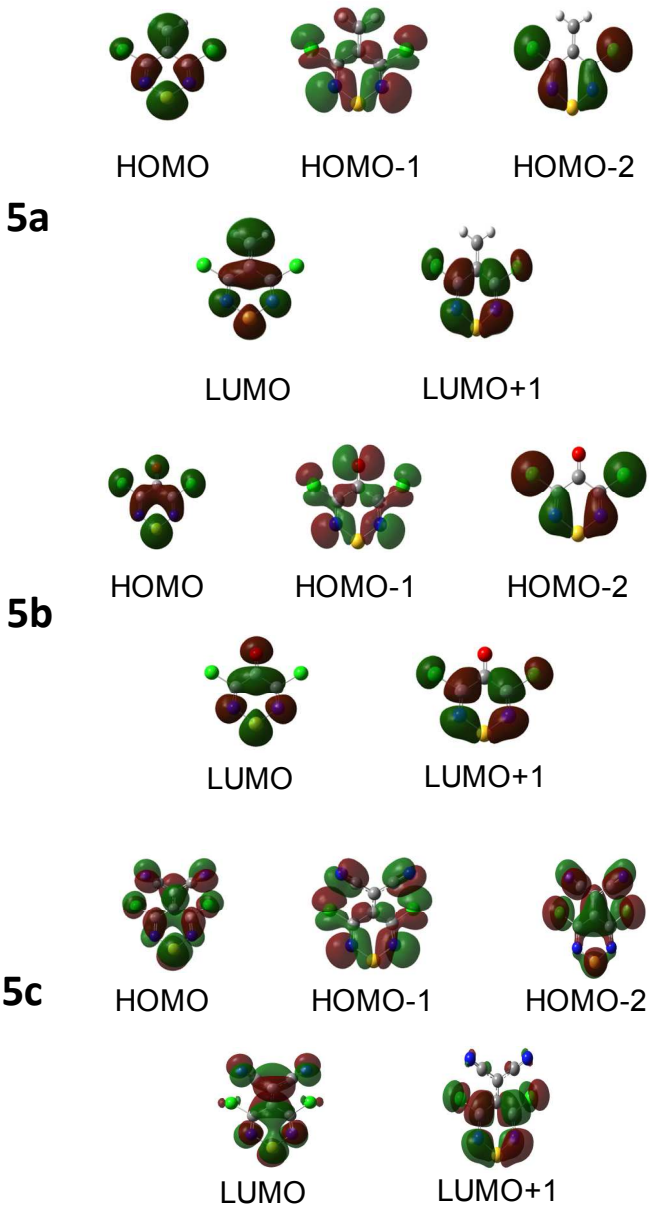

Fig. 8 Frontier MOs for the 4*H*-1,2,6-thiadiazines **5a-c** calculated at the MP2/6-311G(d) level of theory.

2.3. Vibrational analysis of Raman spectra

The resonance Raman spectra of the thiadiazines **5a** (upper), **5b** (middle) and **5c** (bottom) at room temperature are presented in Fig. 9 in the low frequency range (A) and in the range 950-1700 cm^{-1} (B). The spectra were obtained with excitation at 282.4 nm for compounds **5a** and **5b** and 368.9 nm for compound **5c**. Assignment of the vibrational bands was facilitated by normal mode analysis performed using the Gaussian 03 suite of programs at the MP2/6-

311G(d) level of theory.[24] Worthy of note was that the frontier orbitals for the methylene **5a** in Fig. 8 indicated that the two methylene protons have some electron density. As such, the use of a 6-311G(d,p) basis set could better describe this electron density and provide more accurate frequencies. Interestingly, the data obtained from a geometry optimised using the 6-311G(d,p) basis set (data not shown), reproduced the vibrational frequencies to within 1% of the 6-311G(d) calculation.

*3,5-Dichloro-4-methylene-4*H-*1,2,6-thiadiazine (**5a**)*. The most intense band in the spectrum of the methylene **5a** appears at 1589 cm^{-1} and is assigned to the C=C symmetric stretching vibration of the methylene group. The band at 1469 cm^{-1} is assigned to the C=N symmetric stretch and the band at 1555 cm^{-1} to the C=N asymmetric stretch. The latter assignment was based on the large intensity of this band and the absence of the symmetric stretch in the infrared spectrum (see below and ESI) as also predicted from the calculations. A band at 1040 cm^{-1} is attributed to the CH_2 rock of the methylene group, while the CH_2 bend appears at 1378 cm^{-1}. These two assignments were aided by the absence of the analogous frequencies in the Raman spectra of the other two molecules. The band at 1062 cm^{-1} is attributed to the C-C-C symmetric stretch and the band observed at 1256 cm^{-1} is loosely assigned to the C-C-C asymmetric stretch. Identification of the latter band was ambiguous from the normal mode analysis and isotope exchange studies are required for a more convincing assignment. The N-S-N vibrations appear in the low frequency range (Fig. 7A): the ring N-S-N symmetric stretch appears at 825 and the N-S-N bend at 477 cm^{-1}.

Interestingly, a number of bands appearing in the RR spectrum are assigned to asymmetric modes, while only totally-symmetric modes are expected. Such modes can only be observed through Albrecht B term enhancement, which suggests the presence and vibronic coupling of two closely-spaced electronic excited states.[25] This behaviour is observed in all three molecules **5a**, **5b** and **5c**. The electronic structure calculations presented above reveal closely-spaced vertical transitions, which support the experimental findings. In the case of the methylene **5a**, the second absorption band is a weak band that appears around 350 nm as a shoulder to the main absorption band.

Infrared spectra of the compound in the solid state reveal close agreement with the Raman spectra (ESI, Fig. S1). All the experimental and calculated frequencies of the methylene **5a** along with their assignments are listed in Table 2.

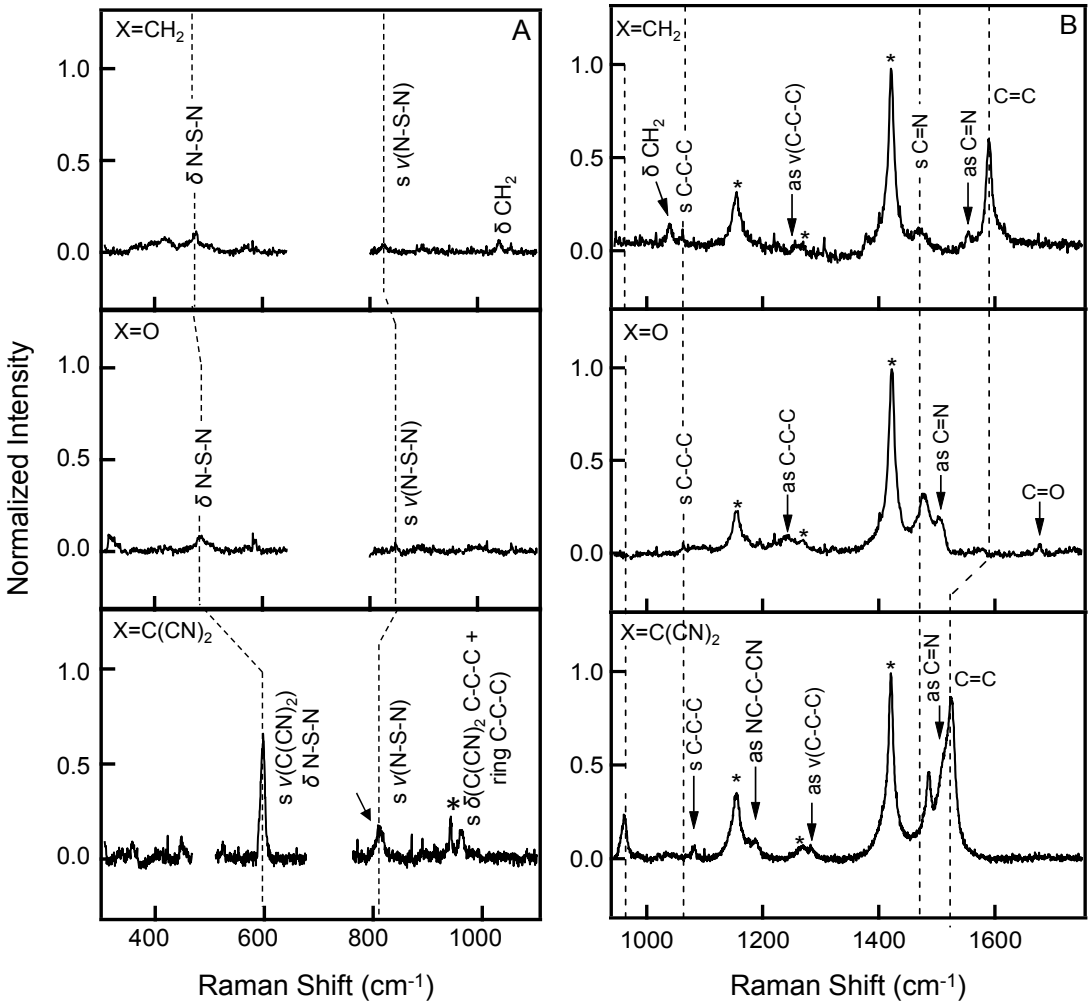

Fig. 9 (A) Resonance Raman (RR) spectra in the low frequency range of the thiadiazines **5a** (upper), and **5b** (middle) excited at 282.4 nm and **5c** (bottom) at 368.9 nm. The intensity scale approximately maintains the band relative intensity with respect to the bands in the high frequency region (B). The gap in the spectra corresponds to the spectral region with the very intense solvent (DCM) bands at 700 and 740 cm^{-1}, and a strong artifact peak at ~500 cm^{-1}. The asterisks correspond to solvent bands or stray scatter.

Table 2 Experimental and MP2/6-311G(d) calculated frequencies of the methylene thiadiazine **5a**

Raman (on resonance) (cm^{-1})	Raman (off resonance) (cm^{-1})	IR (cm^{-1})	MP2/6-311G(d) (cm^{-1})	MP2/6-311G(d) (cm^{-1}) molecule with H	Assignment[a]
364	364		357		s ring breathing/deformation
419	419		376	368	ring bend [op C-C-C (ring), N-S-N & $C(CH_2)$ bend, planar→boat]
477	477		486	445	s N-S-N & C-C-C bend
572	570				n.a.[b]
787	792	792	717		s N-S-N bend/ring deformation
825	827	824	846	674	s N-S-N stretch
861	861		838		CH_2 op bending
1040		1040	1004	987	CH_2 rock
1062		1057	1077	932	s C-C-C (ring) stretch
1194		1192			n.a.[b]
1220	1223				n.a.[b]
1256		1273	1318	1382	as C-C-C (ring) stretch
1289	1289	1290			N-S-N bend + as N-S-N stretch combination
1379		1383	1445	1454	CH_2 s bend (scissoring)
1469	1467		1550	1581	s C=N stretch
1555	1556	1549	1557	1551	as C=N stretch
1589	1590	1587	1638	1653	s C=C stretch and CH_2 bend

[a] s = symmetric, as = asymmetric, ip = in plane, op = out of plane. [b] n.a. = not assigned.

*3,5-Dichloro-4*H-*1,2,6-thiadiazin-4-one (**5b**).* The most intense bands for the thiadiazinone **5b** appear in the range of 1473-1561 cm^{-1} and correspond to the C=N stretching vibrations. The ring symmetric and asymmetric C=N stretch appear at 1478 and 1504 cm^{-1}, respectively. The Raman band for the C=O symmetric stretch of the thiadiazinone **5b** appears at 1678 cm^{-1} as expected for a carbonyl group.[26] The symmetric N-S-N stretch appears at 849 cm^{-1} and the N-S-N bend at 486 cm^{-1}. The band at 1063 cm^{-1} is attributed to the C-C-C symmetric stretch with the in-plane C-C-C asymmetric stretch appearing at 1242 cm^{-1}. There is a close agreement between the bands appearing in the RR and IR spectra for this molecule (see ESI) and the calculated and experimental frequencies with their assignments are listed in Table 3.

Table 3 Experimental and MP2/6-311G(d) calculated frequencies of the thiadiazinone **5b**

Raman (on resonance) (cm^{-1})	Raman (off resonance) (cm^{-1})	IR (cm^{-1})	MP2/6-311G(d) (cm^{-1})	MP2/6-311G(d) (cm^{-1}) molecule with H	Assignment[a]
362			369		ip ring deformation
428	429		446	440	ring bend (op N-S-N & C=O bend) planar→boat
486	486		494	460	s N-S-N & C-C-C bend
	528		513	531	C=O bending + ring deformation
849		854	875	701	s N-S-N stretch
1063	1062	1063	1097	916	s C-C-C (ring) stretch
1221		1225			n.a.[b]
1242	1242	1250	1273	1315	as C-C-C (ring) stretch
1321					n.a.[b]
1478	1477		1461	1519	s C=N stretch
1504	1503	1501	1493	1509	as C=N stretch
1678	1676	1657	1691	1689	s C=O stretch

[a] s = symmetric, as = asymmetric, ip = in plane, op = out of plane. [b] n.a. = not assigned.

*2-(3,5-Dichloro-4*H-*1,2,6-thiadiazin-4-ylidene)malononitrile (**5c**).* Fig. 9 (bottom) depicts the RR spectra of the dicyanomethylene **5c** with excitation at 368.9 nm. The dicyanomethylene group adds new degrees of freedom to this thiadiazine which complicates the spectra. Based

on the normal mode analysis, many of the ring normal modes involve contributions from the substituent in the C-4 position. The most intense band for this compound (1526 cm^{-1}) corresponds to the C=C symmetric stretch of the dicyanomethylene group. The bands corresponding to the C=N symmetric and asymmetric stretching vibrations appear at 1486 and 1512 cm^{-1}, respectively. The mode at 1512 cm^{-1} was deconvolved from the band including the C=C stretch. The band at 962 cm^{-1} is assigned to the C-C-C bending of the dicyanomethylene group in combination with ring C-C-C bending. The symmetric and asymmetric ring C-C-C stretches appear at 1082 and 1283 cm^{-1}, while the band at 1187 cm^{-1} is attributed to C-C-C asymmetric stretching of the dicyanomethylene group. In the range of low frequencies (Fig. 9A, bottom) there are bands due to N-S-N, C-C-C (dicyanomethylene group) and C-C-C (ring) vibrations which appear with enhanced intensity compared to the other two molecules. The N-S-N bend of the dicyanomethylene **5c** appears at 598 cm^{-1} in combination with the symmetric C-C-C bend of the dicyanomethylene moiety, and the symmetric N-S-N stretch appears at 812 cm^{-1}. Finally, the band at 448 cm^{-1} is assigned to a ring bend that involves switching between the boat and the planar conformation. The experimental and calculated vibrational frequencies for the dicyanomethylene **5c**, considering the boat conformation, are listed in Table 4.

Table 4 Experimental and MP2/6-311G(d) calculated frequencies of the dicyanomethylene **5c**

Raman (on resonance) (cm^{-1})	Raman (off resonance) (cm^{-1})	IR (cm^{-1})	MP2/6-311G(d) (cm^{-1})	MP2/6-311G(d) (cm^{-1}) molecule with H	Assignment[a]
358			364	392	ring op bending (boat→planar)
448			456	559	ring op bending (boat→planar)
598			597	624	s C-C-C (dicyano) & N-S-N bend
812	812	812	823	737	s N-S-N stretch
962		966	959	922	C-C-C (dicyano) & C-C-C (ring) bend
1082		1082	1135	981	s C-C-C (ring) stretch

1187			1181	1206	as *v*[C-C-C (dicyano) and C-C-C (ring)]
1283		1288	1319	1404	as *v*[C-C-C (ring) stretch and C-C-C (dicyano)]
1486	1486	1487	1456	1526	s C=N stretch
1512*		1508	1465	1492	as C=N stretch
1525	1525	1522	1567	1596	s C=C stretch
2090			2144	2160	as C-$(C\equiv N)_2$ stretch
2226		2216	2148	2163	s C-$(C\equiv N)_2$ stretch

[a] s = symmetric, as =asymmetric, ip = in plane, op = out of plane, * after deconvolution.

2.4. Structural considerations

The above analysis of the resonance Raman spectra points to distinct differences and similarities in the structure of the three thiadiazines as evidenced by key vibrational modes. The C=N symmetric stretching modes appear systematically at higher frequencies with an increase in the electronegativity of the C-4 substituent *cf.* 1469, 1478, and 1486 cm^{-1} for thiadiazines **5a** (X = CH_2), **5b** (X = O) and **5c** [X = $C(CN)_2$], respectively, signifying an increase in the C=N bond strength and shortening of the bond (Table 5). An increase in frequency was also observed for the ring C-C-C symmetric mode for the most electronegatively-substituted dicyanomethylene **5c** with respect to thiadiazines **5a** and **5b** where it stays almost identical. The latter is in agreement with the calculated frequencies, as well as the increased electron density along the C-C-C bonds seen in the HOMO orbital diagram.

In the low frequency region, the N-S-N bend is one of the most prominent modes. An increasing trend was also observed for the frequency of this normal mode, with a significant increase in the case of the dicyanomethylene **5c** (477, 486, and 595 cm^{-1}, for thiadiazines **5a**, **5b** and **5c**, respectively). In the latter case, normal mode analysis shows two N-S-N bending modes, at 597 and 625 cm^{-1}, both coupled to the dicyanomethylene C-C-C bend but with decreased motion of the sulfur atom. Therefore, it is possible that the mode description is slightly different for the dicyanomethylene **5c**. However, the overall increased strength of the C=N bond with electronegativity could be responsible for the N-S-N bend frequency

increase, as it can hinder the bending motion, thus driving upwards the frequency of this mode.

The N-S-N symmetric stretch depicts a different behaviour; the frequency of the mode increases on going from thiadiazines **5a** to **5b**, but drops significantly in the dicyano-methylene **5c**. This can be tentatively attributed to the change in the ring geometry towards a boat conformation owing to steric interactions between the Cl atoms at the 3 and 5 positions and the bulky dicyanomethylene group that might result in a longer N-S bond. Support for this hypothesis arises from the calculation of the structure and frequencies of all three rings where the chlorine atoms are replaced by hydrogens (Tables 2-5). In this case, the optimized geometry of the rings of all three thiadiazines is planar, and the N-S-N symmetric stretch frequency increases with an increase in the electronegativity of the substituent.

Evidence for delocalization of electron density on going from the methylene **5a** to the dicyanomethylene **5c** comes from the bands corresponding to the C=C symmetric stretch in the C-4 position, where a downshift from 1589 to 1526 cm^{-1} is observed. This delocalization was also supported from the large red shift of both the absorption and fluorescence spectra in the dicyanomethylene **5c**. Interestingly, the delocalization occurs even though the dicyano-methylene **5c** is not planar. The dihedral angles for both the N-S-N and the C-C-C moiety mentioned earlier are, however, shallow enough (< 20^{o}) that orbital overlap is not compromised. Similar observations were reported for deformations of the benzene ring endocyclic torsion angles, where even a 30^{o} deformation retained the topological characteristics of the electron density distribution.[27,28] Furthermore, the study by Shishkin *et al.*,[28] estimates that a 15^{o} deformation from planarity results in an increase in energy of less than 1.5 kcal/mol, suggesting that aromatic rings can possess a significant degree of conformational flexibility while remaining stable. This delocalization of the electron cloud with an increase in the electronegativity of the substituent is further confirmed by the increase in the vibrational frequency of the C-C-C symmetric stretches signifying an increase in the bond order. By analogy, it is expected that the C=N frequency would decrease on going towards a more aromatic system as predicted by computations. Nevertheless, the experimental spectra show a contradictory but small increase of this frequency (~9 cm^{-1} increase at a time, while the difference between the methylene **5a** and the other two rings is ~90 cm^{-1} in the computations). The X-ray data reveal that the C=N bonds are very similar in all three rings, so in the case of the C=N bond the computations have overestimated the bond

length. A similar trend is also found in the computation with the hydrogen atoms, with the methylene C=N bond frequency found much larger than for the other two molecules. The behaviour observed for the C=N mode in the experimental spectra of the rings in solution can be attributed to a balance of various forces occurring upon substitution with an electronegative group. More specifically, if a strongly electronegative substituent group is introduced to the ring, electron density will be drawn away, triggering the chlorines and sulfur to release more electron density to stabilize the ring.

Table 5 Comparison of key vibrational mode frequencies for the three compounds under consideration, both experimentally and theoretically

Vibrational mode	**Experimental ν (cm^{-1})**		
	5a	**5b**	**5c**
C=C	1589	1678 (C=O)	1525
C=N (s, as)	1469/1555	1478/1504	1486/1512
N-S-N δ	477	486	595
N-S-N (s)	825	849	812
C-C-C (s)	1062	1063	1082
Vibrational mode	**Calculated ν (cm^{-1}) (Cl substitution)**		
	5a	**5b**	**5c**
C=C	1638	1691	1567
C=N (s, as)	1550/1557	1461/1493	1456/1465
N-S-N δ	486	494	593
N-S-N (s)	846	873	823
C-C-C (s)	1077	1097	1135
Vibrational mode	**Calculated ν (cm^{-1}) (H substitution)**		
	5a	**5b**	**5c**
C=C	1653	1689	1596
C=N (s, as)	1581/1551	1519/1509	1526/1492
N-S-N δ	445	460	624
N-S-N (s)	674	701	737
C-C-C (s)	932	916	981

The out-of-plane deformability of an aromatic ring and the out-of-plane vibrational frequencies are a sensitive measure of aromaticity in cyclic π-conjugated systems, including heterocyclic compounds such as azines.[27-29] A greater conformational flexibility of a conjugated ring is associated with reduced aromaticity and, consequently, lower out-of-plane vibrational frequencies. In Table 6 the lowest calculated frequencies for a variety of

out-of-plane deformation modes of the three compounds are compared, both with Cl and H substitution. On going from thiadiazine **5a** to **5b** the frequencies of the modes generally increase. In the case of the dicyanomethylene **5c**, however, for each vibrational mode in thiadiazines **5a** and **5b** there are two modes in **5c** that describe the same motion in the ring and which are simultaneously coupled to vibrations in the substituent. Considering the higher frequency mode in this pair, there is a general increase in the out-of-plane vibrational frequencies with an increase in the electronegativity of the substituent at the C-4 position, which can be correlated with the increase in the aromaticity of a cyclic π-conjugated system.

Table 6 MP2/6-311G(d) calculated frequencies for out-of-plane deformation normal modes of thiadiazines **5a**, **5b**, and **5c**

Calculated ν (cm^{-1})			Assignment
5a	**5b**	**5c**	
18	54	132	op C-C-C ring bend
195	194	186/224	op C-C-C(ring)/N-S-N deformation
376	445	364/456	ring bend [op C-C-C (ring), N-S-N bend, planar→boat]
Calculated ν (cm^{-1}) (H substitution)			
60	105	60/179	op C-C-C ring bend
368	440	392/559	ring bend [op C-C-C (ring), N-S-N bend, planar→boat]
387	385	387/440	op C-C-C(ring)/N-S-N deformation

The above observations are in line with the statistical evaluation of deviations in peripheral bond orders derived from crystallographically determined bond lengths within the ring,[30,31] which indicated that thiadiazine **5a** has a low Bird's aromaticity index $I_A = 45$, while those of the analogous thiadiazinone **5b** and the dicyanomethylene **5c** are 54 and 60,[4,6] respectively [*cf.* furan ($I_A = 53$) and benzene ($I_A = 100$)].[24,25] This supports an aromaticity order across the three analogues of **5a** ($X = CH_2$) < **5b** ($X = O$) < **5c** [$X = C(CN)_2$], which is in line with the relative electron withdrawing power of the C-4 substituents and the stability of the rings. The more strongly electron withdrawing C-4 substituents [O and $C(CN)_2$] presumably enable a

greater contribution of resonance forms like **I**, and even **II**, to the overall electronic structure (Scheme 2).

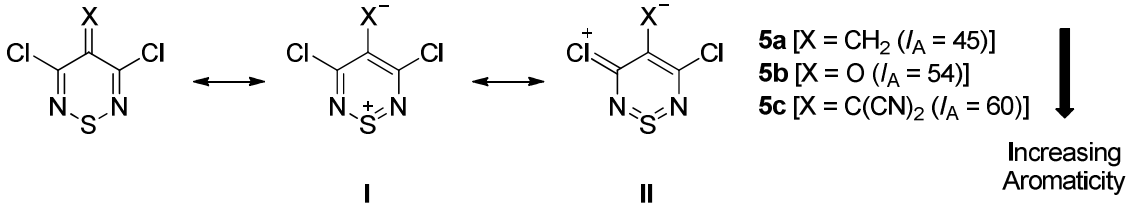

Scheme 2 Resonance structures of 3,5-dichloro-4*H*-1,2,6-thiadiazines **5a-c**

The influence of the electronegativity of a substituent on the structure and electronic properties of an electron-poor heterocycle is important within the organic semiconductor community that seeks new opportunities for improving the optoelectronic properties of push-pull materials employed in photovoltaic devices. Some of the most efficient polymeric materials currently under investigation include electron acceptor molecules with the N-S-N moiety.[32] Therefore, a salient question would be whether the ring system investigated in this study can be useful as potential component in push-pull compounds. Introducing a strong electron withdrawing group at the C-4 position of the thiadiazine such as the dicyano-methylene improves the electron affinity of the ring system but unfavourable steric interactions of this bulky substituent with the chlorines in the 3 and 5 position leads to deformation of the ring system. Despite this ring deformation, the overall aromaticity of the dicyanomethylene **5c** improves. Electrochemical studies on the three molecules investigated here showed that indeed the dicyanomethylene **5c** has the best prospects as an electron acceptor owing to the low LUMO energy.[19]

3. Conclusion

The present study focused on the effect of C-4 substitution on the structure and electronic properties of 3,5-dichloro-4*H*-1,2,6-thiadiazine rings, investigated with absorption, fluorescence and Resonance Raman spectroscopy. The combined evidence suggests that increase in the electronegative nature of the substituent leads to delocalization of the electron cloud and increased aromaticity of the ring, despite the slight deviation of the dicyanomethylene **5c** ring from planarity.

4. Experimental

4.1. Synthesis

4.1.1. General Procedures. Et_2O was distilled over CaH_2. Anhydrous Na_2SO_4 was used for drying organic extracts and all volatiles were removed under reduced pressure. All reaction mixtures and column eluents were monitored by TLC using commercial glass backed thin layer chromatography (TLC) plates (Merck Kieselgel 60 F_{254}). The plates were observed under UV light at 254 and 365 nm. The technique of dry flash chromatography was used throughout for all non-TLC scale chromatographic separations using Merck Silica Gel 60 (less than 0.063 mm).[33] Melting points were determined using a PolyTherm-A, Wagner & Munz, Koefler-Hotstage Microscope apparatus. Solvents used for recrystallization are indicated after the melting point. Initial UV spectra were obtained using a Perkin-Elmer Lambda-25 UV/vis spectrophotometer. IR spectra were recorded on a Shimadzu FTIR-NIR Prestige-21 spectrometer with Pike *Miracle* Ge ATR accessory and strong, medium and weak peaks are represented by s, m and w, respectively. ^{1}H and ^{13}C NMR spectra were recorded on a Bruker Avance 500 machine (at 500 and 125 MHz, respectively). Deuterated solvents were used for homonuclear lock and the signals are referenced to the deuterated solvent peaks. Low resolution (EI) mass spectra were recorded on a Shimadzu Q2010 GCMS with direct inlet probe. 3,5-Dichloro-4*H*-1,2,6-thiadiazin-4-one (**5b**)[3] and 2-(3,5-dichloro-4*H*-1,2,6-thiadiazin-4-ylidene)malononitrile (**5c**)[8] were prepared according to literature procedures.

*4.1.2. 3,5-Dichloro-4-methylene-4*H*-1,2,6-thiadiazine* (**5a**). To a flask containing 3,5-dichloro-4*H*-1,2,6-thiadiazin-4-one (**5b**) (370 mg, 2.02 mmol) and dry Et_2O (4 ml) under argon at -78 ^oC, was added MeMgBr (2.9 ml, 2 equiv) and the mixture was stirred at this temperature until no starting material remained (TLC). The reaction mixture was then quenched with saturated NH_4Cl and extracted (DCM). The organic layer was washed with brine, dried and evaporated. The resulting product (402 mg, 100%) was dissolved in PhMe (4 ml) and *p*-TsOH·H_2O (38 mg, 0.202 mmol) was added and the mixture was heated at *ca.* 110 ^oC until no starting material remained (TLC). The reaction mixture was adsorbed onto silica and chromatography (*n*-hexane/DCM, 7:3) gave the *title compound* **5a** (183 mg, 50%) as yellow needles, mp 73-75 ^oC (from *n*-pentane, 0 ^oC); R_f 0.48 (*n*-hexane/DCM, 7:3); (Found: C, 26.63; H, 1.05; N, 15.40. $C_4H_2Cl_2N_2S$ requires C, 26.54; H, 1.11; N, 15.47%); λ_{max}(DCM)/nm 230 (log ε 3.06), 309 (3.72); ν_{max}/cm^{-1} 3132w, 3030w, 1838w, 1587w, 1549s, 1383w, 1290m, 1273s, 1192w, 1057w, 1040m, 980s, 916s, 824w, 793w; δ_H(500 MHz;

$CDCl_3$) 6.11 (2H, s, CH_2); δ_C(125 MHz; $CDCl_3$) 145.3 (s), 125.3 (s), 120.1 (CH_2); *m/z* (EI) 184 (M^++3, 7%), 182 (M^++1, 34), 180 (M^+-1, 47), 147 (43), 145 (100), 118 (4), 109 (19), 93 (12), 84 (17), 82 (9), 67 (13), 58 (13).

4.2. Electronic spectroscopy

The absorption spectra were recorded on a JASCO V-530 UV-visible spectrophotometer and fluorescence spectra were obtained after excitation at the corresponding $\lambda_{abs,max}$ on a JASCO FP-6300 spectrofluorometer. Solutions of the compounds **5a-c** were prepared in dichloromethane with concentrations of the order of 10^{-4} M ([**5a**] = 6.6 × 10^{-4}, [**5b**] = 5.5 × 10^{-4}, [**5c**] = 3.9 × 10^{-4} mol.L^{-1} for absorption and RR measurements and for fluorescent measurements [**5a**] = 5.5 × 10^{-4}, [**5b**] = 5.5 × 10^{-4}, [**5c**] = 4.3 × 10^{-4} mol.L^{-1}). Dichloromethane was of HPLC grade (Aldrich) and used as received.

4.3. Resonance Raman spectroscopy

RR measurements were performed using a homebuilt system described elsewhere.[34] Briefly, the excitation wavelengths in the region of interest are produced *via* Raman shifting of the second harmonic from a Q-switched Nd:YAG laser at 532 nm and using the 2nd and 4th anti-Stokes line at 368.91 and 282.35 nm, respectively. The excitation light was focused into a spinning cell, consisting of an EPR quartz tube (diameter: 4 mm), attached to a rheostat-controlled motor for choice of rotation speed. Use of the spinning cell prolonged the lifetime of the samples, as no degradation was observed after 1 h, at which point a fresh sample was used. The Raman scattered light was collected in a backscattering geometry and delivered to a 0.75 m focal-length Czerny-Turner spectrograph, equipped with a 2400-grooves/mm UV-enhanced holographic grating. The slit width was set to 100 μm providing for 4 and 6.5 cm^{-1} spectral resolution at the wavelengths used in this work (λ = 368.91 and 282.35 nm, respectively). The scattered light was detected by a LN_2-cooled 2048 × 512 pixel, back-illuminated UV-enhanced CCD detector (Spec10:2KBUV/LN, Princeton Instruments). Frequency calibration was accomplished with the use of toluene at 368.91 nm and cyclohexane at 282.35 nm. MATLAB was used for spectral treatment and analysis.

4.4. Computational procedures

The geometry of each system was fully optimized using the MP2/6-311G(d) methods which gave reasonable comparison of X-ray determined bond lengths and angles for all three

structures. Raman frequencies were calculated at the same level of theory for each optimized structure. Time-dependent calculations were implemented using TD-DFT/B3LYP/6-311+G(2d) method on the MP2/6-311G(d) optimized structures. All the above computations were performed using the Gaussian 03 suite of programs.[24]

4.5. X-ray crystallographic studies

Data were collected on an Oxford-Diffraction Supernova diffractometer, equipped with a CCD area detector utilizing Cu-Kα radiation (λ = 1.5418 Å). A suitable crystal was attached to glass fibers using paratone-N oil and transferred to a goniostat where they were cooled for data collection. Unit cell dimensions were determined and refined by using 957 ($4.64 \leq \theta \leq 66.95^{o}$) reflections. Empirical absorption corrections (multi-scan based on symmetry-related measurements) were applied using CrysAlis RED software.[35] The structures were solved by direct method and refined on F[36] using full-matrix least squares using SHELXL97.[36] Software packages used: CrysAlis CCD[35] for data collection, CrysAlis RED[35] for cell refinement and data reduction, WINGX for geometric calculations,[37] and DIAMOND[38] for molecular graphics. The non-H atoms were treated anisotropically. The hydrogen atoms were placed in calculated, ideal positions and refined as riding on their respective carbon atoms.

Crystal refinement data for compound ***5a***. $C_4H_2Cl_2N_2S$, M = 181.04, Monoclinic, space group *P 21/c*, a = 3.8127(5) Å, b = 17.606(2) Å, c = 9.6396(15) Å, $\alpha = 90^{o}$, β = 99.086(14)^{o}, $\gamma = 90^{o}$, V = 638.96(15) Å^3, Z = 4, T = 100(2) K, ρ_{calcd} = 1.882 g cm^{-3}, $2\theta_{max}$ = 67. Refinement of 82 parameters on 1129 independent reflections out of 2048 measured reflections (R_{int} = 0.0353) led to R_1 = 0.0474 [I>2s(I)], wR_2 = 0.1434 (all data), and S = 1.089 with the largest difference peak and hole of 0.679 and -0.414 e^{-3}, respectively.

Crystallographic data for compound **5a** has been deposited with the Cambridge Crystallographic Data Centre with deposit numbers CCDC-1038262. This data can be obtained free of charge *via* www.ccdc.cam.ac.uk/data_request/cif (or from the Cambridge Crystallographic Data Centre, 12 Union Road, Cambridge CB2 1EZ, UK; fax: +44 1223 336033; or e-mail: deposit@ccdc.cam.ac.uk).

Acknowledgements

The authors thank the Cyprus Research Promotion Foundation [Grant Nos. NEKYΠ/0308/02, ΣTPATHII/0308/06, TEXNO/0104/04 and ENIΣX/0504/08], the University of Cyprus for a

Medium Sized Research Grant, and the following organisations in Cyprus for generous donations of chemicals and glassware: the State General Laboratory, the Agricultural Research Institute, the Ministry of Agriculture, MedoChemie Ltd, Medisell Ltd and Biotronics Ltd. Finally, we thank the A.G. Leventis Foundation for helping to establish the NMR facility in the University of Cyprus.

Electronic Supplementary Information (ESI) available: Comparison of IR and resonance Raman spectra of thiadiazines **5a-c** (Figure S1). Atomic coordinates of the geometry optimized structures of thiadiazines **5a-c** and their H analogues using MP2/6-311G(d). Comparison of bond lengths and angles of thiadiazines **5a-c** from single crystal X-ray structures and geometry optimizations. See DOI:10.1039/b000000x/

References

1. A. R. Katritzky and A. F. Pozharskii, *Handbook of Heterocyclic Chemistry*, 2nd edn., Pergamon Press, Oxford, 2000.
2. S. P. Economopoulos, G. Itskos, P. A. Koutentis and S. A. Choulis, *Overview of Polymer and Copolymer Materials for Organic Photovoltaics*, 2nd edn., Wiley-VCH Verlag GmbH & Co. KGaA., 2014.
3. J. Geevers and W. P. Trompen, *Recl. Trav. Chim. Pays-Bas*, 1974, **93**, 270-272.
4. C. J. Peake, W. N. Harnish and B. L. Davidson, *U.S. Patent* 4,097,594, 1978**.**
5. M. P. Cava, M. V. Lakshmikantham, R. Hoffmann and R. M. Williams, *Tetrahedron*, 2011, **67**, 6771-6797.
6. P. A. Koutentis, C. W. Rees, A. J. P. White and D. J. Williams, *Chem. Comm.*, 2000, 303-304.
7. P. A. Koutentis and C. W. Rees, *J. Chem. Soc., Perkin Trans. 1*, 2000, 2601-2607.
8. P. A. Koutentis and C. W. Rees, *J. Chem. Soc., Perkin Trans. 1*, 2000, 1089-1094.
9. P. Flowerday and M. J. Perkins, *Tetrahedron Lett.*, 1968, **9**, 1261-1264.
10. P. Flowerday, M. J. Perkins and A. R. J. Arthur, *J. Chem. Soc. C*, 1970, 290-297.
11. R. C. Haddon, M. L. Kaplan and J. H. Marshall, *J. Am. Chem. Soc.*, 1978, **100**, 1235-1239.
12. S. Macho, D. Miguel, T. Gomez, T. Rodriguez and T. Torroba, *J. Org. Chem.*, 2005, **70**, 9314-9325.

13. S. Macho, D. Miguel, A. G. Neo, T. Rodriguez and T. Torroba, *Chem. Comm.*, 2005, 334-336.
14. P. A. Koutentis and C. W. Rees, *J. Chem. Soc., Perkin Trans. 1*, 2000, 1081-1088.
15. A. S. Kalogirou, P. A. Koutentis and M. D. Rikkou, *Tetrahedron*, 2010, **66**, 1817-1820.
16. H. A. Ioannidou, C. Kizas and P. A. Koutentis, *Org. Lett.*, 2011, **13**, 3466-3469.
17. H. A. Ioannidou, C. Kizas and P. A. Koutentis, *Org. Lett.*, 2011, **13**, 5886-5889.
18. H. A. Ioannidou and P. A. Koutentis, *Tetrahedron*, 2012, **68**, 2590-2597.
19. S. P. Economopoulos, P. A. Koutentis, H. A. Ioannidou and S. A. Choulis, *Electrochim. Acta*, 2013, **107**, 448-453.
20. F. Hermerschmidt, A. S. Kalogirou, J. Min, G. A. Zissimou, S. M. Tuladhar, T. Ameri, H. Faber, G. Itskos, S. A. Choulis, T. D. Anthopoulos, D. D. C. Bradley, J. Nelson, C. J. Brabec and P. A. Koutentis, *J. Mat. Chem. C*, 2015, DOI: 10.1039/c4tc02931c.
21. S. Harkema, *Acta Crystallogr.*, *Sect. B: Struct. Crystallogr. Cryst. Chem.*, 1978, **34**, 2927-2928.
22. R. P. Ortiz, J. Casado, V. Hernández, J. T. L. Navarrete, J. A. Letizia, M. A. Ratner, A. Facchetti and T. J. Marks, *Chem. –Eur. J.l*, 2009, **15**, 5023-5039.
23. Personal communication with C. Walter, 2014.
24. G. W. T. M. J. Frisch, H. B. Schlegel, G. E. Scuseria, M. A. Robb, J. R. Cheeseman, Jr. J. A. Montgomery, T. Vreven, K. N. Kudin, J. C. Burant, J. M. Millam, S. S. Iyengar, J. Tomasi, V. Barone, B. Mennucci, M. Cossi, G. Scalmani, N. Rega, G. A. Petersson, H. Nakatsuji, M. Hada, M. Ehara, K. Toyota, R. Fukuda, J. Hasegawa, M. Ishida, T. Nakajima, Y. Honda, O. Kitao, H. Nakai, M. Klene, X. Li, J. E. Knox, H. P. Hratchian, J. B. Cross, V. Bakken, C. Adamo, J. Jaramillo, R. Gomperts, R. E. Stratmann, O. Yazyev, A. J. Austin, R. Cammi, C. Pomelli, J. W. Ochterski, P. Y. Ayala, K. Morokuma, G. A. Voth, P. Salvador, J. J. Dannenberg, V. G. Zakrzewski, S. Dapprich, A. D. Daniels, M. C. Strain, O. Farkas, D. K. Malick, A. D. Rabuck, K. Raghavachari, J. B. Foresman, J. V. Ortiz, Q. Cui, A. G. Baboul, S. Clifford, J. Cioslowski, B. B. Stefanov, G. Liu, A. Liashenko, P. Piskorz, I. Komaromi, R. L. Martin, D. J. Fox, T. Keith, M. A. Al-Laham, C. Y. Peng, A. Nanayakkara, M. Challacombe, P. M. W. Gill, B. Johnson, W. Chen, M. W. Wong, C. Gonzalez, J. A. Pople, Gaussian, Inc., Wallingford CT, 2004.

25. J. L. McHale, *Molecular Spectroscopy*, Prentice Hall, 1998.
26. R. M. Silverstein, F. X. Webster and D. Kiemle, *Spectrometric Identification of Organic Compounds*, 7th edn., John Wiley and Sons, New York, NY, USA, 2005.
27. O. V. Shishkin, I. V. Omelchenko, M. V. Krasovska, R. I. Zubatyuk, L. Gorb and J. Leszczynski, *J. Mol. Struct.*, 2006, **791**, 158-164.
28. O. V. Shishkin, K. Y. Pichugin, L. Gorb and J. Leszczynski, *J. Mol. Struct.*, 2002, **616**, 159-166.
29. I. V. Omelchenko, O. V. Shishkin, L. Gorb, J. Leszczynski, S. Fias and P. Bultinck, *Phys. Chem. Chem. Phys.*, 2011, **13**, 20536-20548.
30. C. W. Bird, *Tetrahedron*, 1986, **42**, 89-92.
31. C. W. Bird, *Tetrahedron*, 1992, **48**, 335-340.
32. P. A. Koutentis, in *Comprehensive Heterocyclic Chemistry III*, ed. V. V. Zhdankin, 2008, vol. 5, pp. 515-565.
33. L. M. Harwood, *Aldrichimica Acta*, 1985, **18**, 25.
34. G. K. Pieridou and S. C. Hayes, *Phys. Chem. Chem. Phys.*, 2009, **11**, 5302-5309.
35. O. Diffraction, *CrysAlis CCD and CrysAlis RED*, (2008) Oxford Diffraction Ltd, Abingdon, Oxford, England.
36. G. M. Sheldrick, *SHELXL97dA Program for the Refinement of Crystal Structure*, (1997), University of Göttingen: Germany.
37. L. Farrugia, *J. Appl. Crystallogr.*, 1999, **32**, 837-838.
38. K. Brandenburg, *DIAMOND*, (2006) Crystal Impact GbR, Bonn, Germany.